

Estimation of Present Prestressing Force in Existing Prestressed Concrete Bridge

MAJOR PROJECT-II (4th Semester)

MASTERS OF TECHNOLOGY
IN
CIVIL ENGINEERING
(Structural Engineering)

Submitted By
KUMAR SHASHI BHUSHAN
(Roll No-2K15/STE/09)

Under the Guidance of

Co-supervisor

Dr. Rajeev Goel
Senior Principal Scientist
CSIR-Central Road Research Institute, New Delhi

Supervisor

Dr. Awadhesh Kumar
(Associate Professor)
Delhi Technological University, New Delhi



**Delhi Technological University
Bawana Road, New Delhi-110042**

June 2017

CANDIDATE'S DECLARATION AND CERTIFICATE

This is to declare that the project entitled “**Estimation of Present Prestressing Force in Existing Prestressed Concrete Bridge**” is a record of work done by me under the guidance of Dr. Awadhesh Kumar, Associate Professor, Delhi Technical University, Bawana Road, New Delhi and Dr. Rajeev Goel, Senior Principal Scientist, CSIR-Central Road Research Institute, New Delhi, for the partial fulfillment of the requirements of the Degree of Master of Technology in Civil Engineering (Structural Engineering), Delhi Technical University, Bawana Road, New Delhi-110042

The matter embodied in this report is original and has not been submitted for the award of any other degree or diploma.

Date: 29.06.2017

.....
Kumar Shashi Bhushan

(Roll No: 2K15/STE/09)

This is to certify that the above statement made by the candidate is correct to the best of my knowledge.

.....
Dr. Awadhesh Kumar
Associate Professor
Delhi Technological University
New Delhi

ACKNOWLEDGEMENT

I wish to express my deep sense of gratitude and appreciation to Dr. Awadhesh Kumar, Associate Professor, Delhi Technological University, New Delhi, for his guidance and valuable advice throughout this project without which the completion of this project would have not been possible.

I pay my sincere thanks to Director, CSIR-Central Road Research Institute, New Delhi, for his kind approval to allow me to carry out the project work with the institute. Sincerely, I thank my project guide Dr. Rajeev Goel, Senior Principal Scientist, Dr. Rajeev Kumar Garg, Chief Scientist and Er. Ganesh Kumar Sahu, Senior Principal Scientist, CSIR-Central Road Research Institute, New Delhi for giving me valuable & inspiring guidance and excellent advice during the project work and for giving support in preparation of report.

I extend my gratitude to Dr. Lakshmy P, Chief Scientist, CSIR-Central Road Research Institute for giving inspiration at need. I pay my thanks to Er. S. S. Gaharwar, Senior Principal Scientist & HOD-BES Division, CSIR-Central Road Research Institute for giving valuable guidance. I also thank Sh. Yogendra Kumar Singh, Senior Technical Officer, Sh. Pardeep Kumar Hans, Senior Technical Officer and Sh. Sushil Kumar, Principal Technical Officer, Sh. Rajveer Singh, Technician, BES Division, CSIR-Central Road Research Institute, New Delhi for their dedicated support in carrying out the project and their constant generous help and cooperation throughout my project work.

Lastly but not least, I would like to pay sincere thanks to my mother, Dr. Krishna Pandey & my father, Sh. Hardwar Pandey, for their constant blessings in conducting this work, my wife, Mrs. Priyanka Bhushan and special thanks to my children, Yash and Mahima along with my friends without their love, affection and moral support, it would have been impossible to accomplish the job.

(Kumar Shashi Bhushan)

ABSTRACT

Prestressed Concrete (PSC) structures especially bridges are being largely used all over the world due to their multifarious advantages in terms of structural behaviour, economy as well as aesthetical aspects. However, many PSC structures deteriorate with time due to several factors which may lead to certain loss in their initial applied prestress. This loss may affect the structure behaviour and its service life adversely and need to be checked. Such loss of prestress will also result degradation in stiffness of the structure. A precise determination of prestress losses in prestressed concrete members is a complicated problem because the rate of loss due to one factor, such as relaxation of prestressing cables, is continually being altered by changes in stress due to other factors, such as creep of concrete. It has been known that any change in the stiffness of the structure will change its natural frequency also. Hence, it may be possible to ascertain the loss by measurement of natural frequency at regular intervals.

In this study, an effort has been made to determine the natural frequency of a PSC structure by carrying out Vibration Study on it and determining the existing prestressing force to ascertain the loss of prestress. To achieve this objective, following methodology has been adopted:

1. The theoretical study has been carried out to establish a relationship between natural frequency and prestressing force for a simply-supported prestressed concrete bridge of composite section having parabolic profile of prestressing cables.
2. Experimental study has been carried out to determine the natural frequency of the bridge and measurement of prestressing force, using load cells which were installed during the construction of the bridge.
3. Thereafter, present prestressing force has been estimated using the developed relationship between natural frequency and prestressing force.
4. Results of estimated prestressing force were then compared with the measured prestressing force.

NOMENCLATURE

A_c	Area of concrete in beam cross section
A_s	Area of steel in beam cross section
b_f	Width of flange in T-beam
b_w	Width of web in T-beam
C	Damping
d_f	Depth of flange in T-beam
d_w	Depth of web in T-beam
dP	Change in prestressing force
dM_p	Additional moment due to prestressing force
d_{3x}^2	wave number that depends on mass density and Young's modulus of the piezoelectric material
E_c	Modulus of elasticity of concrete
E_s	Modulus of elasticity of steel
E_r	Modulus of elasticity of composite structure
EI	Flexural rigidity of beam
$e(x)$	Eccentricity of prestressing cable from neutral axis
e_o	Maximum eccentricity of prestressing cable
F	Fundamental natural frequency of beam
f_{ck}	Compressive strength of concrete
$H(f)$	Frequency response function
I_c	Moment of inertia of concrete
I_e	Effective moment of inertia
I_s	Moment of inertia of steel
I_r	Moment of inertia of composite section
K_i	Modal stiffness
$K(x)$	Bending stiffness of beam
K	Curvature at any point in the cross-section of beam
K	wave number that depends on mass density and Young's modulus of the piezoelectric material
L	Length of the beam

L_r	Change in length of the beam
M	Bending moment of beam
m_r	Mass per unit length of the beam of composite section
M_p	Moment due to prestressing force
N	Prestressing force
P	Prestressing force
R	Reaction at supports
T_{max}	Maximum kinetic energy
$U(f)$	Force transformed into frequency
$V(f)$	Displacement transformed into frequency
V_{max}	Maximum potential energy
W_1	Equivalent weight on span 1 of T-beam
W_2	Equivalent weight on span 2 of T-beam
$Y(x)$	Deformed vertical shape function of the beam
$Y(\omega)$	electrical admittance (the inverse of electro-mechanical impedance) of the patch
Y_{XX}	complex Young's modulus of the at zero electric field
$Z_a(\omega)$	piezoelectric patch
$Z_s(\omega)$	host structure
$\rho(x)$	Mass per unit length
ρ_c	Density of concrete
ρ_s	Density of steel
$\phi_I(x)$	Mode shape of the beam
A	Curvature of prestressing cable profile
Δ	Difference in absolute curvatures of the undamaged and damaged structures
γ	Weight per unit length of the beam
φ	Modal displacement
ϵ_{33}^T	Dielectric constant of piezoelectric wafer
ω_n	nth natural frequency of the beam

TABLE OF CONTENTS

S. No.		Page No.
Chapter-1 INTRODUCTION		
1.1	General	12
1.2	Prestressed Concrete over Reinforced Concrete	12
1.3	Post tensioned Concrete	13
	1.3.1: Un-bonded System	13
	1.3.2: Bonded System	14
1.4	Prestress Loss	
	1.4.1: Type of Prestress Loss	15-16
1.5	Statement of the Problem	17
1.6	Objective of the Study	17
1.7	Organization of thesis	17
Chapter-2 LITERATURE REVIEW		
2.1	Introduction	20
2.2	Review of Research	20-26
2.3	Techniques of calculating Prestressing Force	26
	2.3.1: Vibration based damaged detection technique	26
	2.3.1.1: Prestress loss prediction model	26
	2.3.1.2: Mode shape based crack detection method	27
	2.3.1.3: Acceleration based method	27
	2.3.1.4: Impedance based method	28
	2.3.1.5: Rayleigh's method	29
	2.3.1.6: Simply supported beam with parabolic profile	30
	2.3.1.6: Mode shape curvature/strain mode shape change	33
	2.3.1.7: Methods based on dynamically measured flexibility	34
	2.3.2: Distributed optical fiber sensing technique	35
	2.3.3: Instrumentation techniques	35

Chapter-3	METHODOLOGY	
3.1	Introduction	37
3.2	Experimental Studies	37
	3.2.1:Structure Detail	38
	3.2.2: Experimental Program-I	42
	3.2.2: Experimental Program-II	45
3.3	NDTs of the structure	50
3.4	Theoretical analysis of Prestressed Beam	55
Chapter-4	RESULTS &DISCUSSIONS	
4.1	Experimental Result-I	
	4.1.1: Experiment-I	59
	4.1.2: Experiment-II	60
	4.1.3: Theoretical and experimental Result	65
Chapter-5	CONCLUSIONS	
	5.1: Conclusions	68
	5.2: Recommendations for future work	69
	<i>References</i>	70
	<i>Annexure (Load Cell Calibration Certificates)</i>	71-74

LIST OF FIGURES / TABLES / GRAPHS / PHOTOS

S. No	Description of Figure/Photo/Graph/Table	Page No.
A. FIGURES:		
	Fig-1.1: Stress in Concrete when Prestress is applied at the C.G. of the section	12
	Fig-1.2: Unbounded Prestressing cable System	14
	Fig-1.3: Bonded Prestressing cable System	14
	Fig-1.4: Types of Prestress Losses	16
	Fig-2.1: Prestress loss prediction result for PSC girder	22
	Fig-2.2: Results of damage location for each damage case in PSC girder	22
	Fig-2.3: Tensile strength of Model of PSC beam	26
	Fig-2.4: Layout of prestressed simply supported beam	30
	Fig.2.5: Element of beam with and without prestressing cables	31
	Fig-3.1: Cross section at support	38
	Fig-3.2: Details of cable-1 and cable-3 in PSC girder bridge	40
	Fig-3.3: Details of cable-2 and cable-4 in PSC girder bridge	40
	Fig-3.4: Location detail of Accelerometers on top of RCC slab of bridge model	45
	Fig-3.5: Natural Frequency measurement scheme	47
B. TABLES:		
	Table-1.1: Type of Losses in various prestressing system	16
	Table-3.1: Reading from Load Cells	43
	Table-3.2: Initial and Existing Prestressing Force	44
	Table-3.3: Rebound Hammer values for Surface Hardness of Bridge Girder	51
	Table-3.4: UPV Test values for Bridge Girder	53
	Table-4.1: Initial and Existing Prestressing Force	59
	Table-4.2: Values of Loss of Prestress	60
	Table-4.3: Theoretical and Experimental First Natural Frequency	65
	Table-4.4: Prestressing force in cables w.r.t. theoretical natural frequency	66
C. GRAPHS:		
	Graph-4.1: Time vs Acceleration Graph in time domain for all accelerometers	61
	Graph-4.2: Spectrum of the Vertical Vibration at U/s Support (Input-1)	61
	Graph-4.3: Spectrum of the Vertical Vibration at D/s Support (Input-3)	62
	Graph-4.4: Spectrum of the Vertical Vibration at U/s Qtr span (Support side, Input-4)	62

Graph-4.5: Spectrum of the Vertical Vibration at Centre, Qtr span (Support side, Input-5)	62
Graph-4.6: Spectrum of the Vertical Vibration at D/s Qtr span (Support side, Input-6)	63
Graph-4.7: Spectrum of the Vertical Vibration at U/s Mid Span (Input-7)	63
Graph-4.8: Spectrum of the Vertical Vibration at Centre of Mid Span (Input-8)	63
Graph-4.9: Spectrum of the Vertical Vibration at D/s Mid Span (Input-9)	64
Graph-4.10: Spectrum of the Vertical Vibration at U/s Quarter Span (Input-10)	64
Graph-4.11: Spectrum of the Vertical Vibration at U/s Centre of Qtr Span (Input-11)	64
Graph-4.12: Spectrum of the Vertical Vibration at D/s Quarter Span (Input-12)	65

D. PHOTOS:

Photo-3.1: Complete view of Single span Composite PSC Girder	38
Photo-3.2: Vibrating wire (VW) Load Cell	41
Photo-3.3: Vibrating wire (VW) Load cell arrangement	42
Photo-3.4: Connecting wires of load cells to take reading through GK-403	43
Photo-3.5: Reading output from load cells through GK-403	43
Photo-3.6: Instruments used in experimental study	46
Photo-3.7: Fixing of Accelerometers on top surface of Composite PSC girder	48
Photo-3.8: Beam subjected to vibration study by giving an impact with hammer at Qtr span	49
Photo-3.9: Beam subjected to vibration study by giving an impact with hammer at mid span	49
Photo-3.10: A view of performing Rebound Hammer Test	50
Photo-3.11: A view of performing Rebound Hammer Test	50
Photo-3.12: A view of Performing UPV Test of RCC Slab	52
Photo-3.13: A view of Performing UPV Test of RCC Slab	52
Photo-3.14: A view of Performing Carbonation Test	54
Photo-3.15: A view of Performing Carbonation Test	54

CHAPTER-1

INTRODUCTION

1.1 GENERAL

As the concrete is weak in taking tensile forces, so in reinforced concrete (RCC) structures, steel reinforcement bars are used to take tension in those locations of the member where tension may arise, compensating for the low tensile strength of the concrete. In practice, reinforced concrete structures are designed by assuming that cracks will occur in concrete under their service loads. This is not the case in a prestressed concrete beam.

In prestressed concrete (PSC) structures, prestressing is done to add an initial compressive axial force to the concrete which highly reduces or eliminates the internal tensile stresses (see Fig. 1.1). This is done by providing the tensile stress to prestressing cable, passing through the concrete. The prestressing cable is then anchored at the ends. By this, a compressive force is transferred to the concrete.

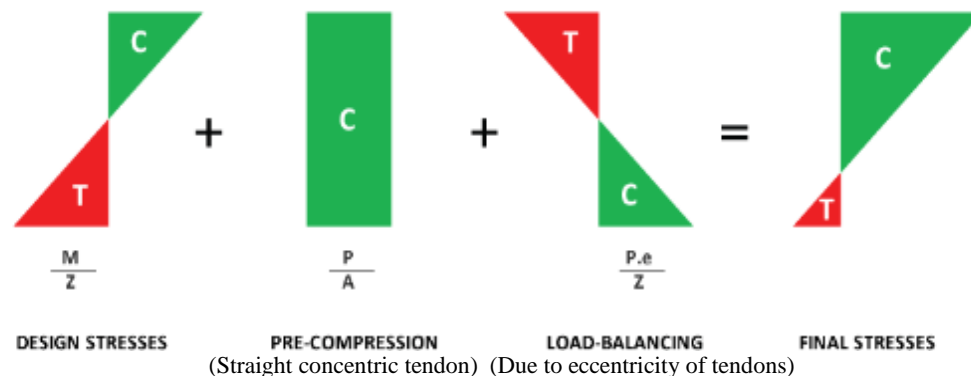


Fig. 1.1: Combined effect of stress in prestressed concrete

1.2 ADVANTAGES AND DISADVANTAGES OF PSC OVER RCC

Advantages of prestressed concrete over reinforced concrete structures are:

- Cracking is highly reduced or eliminated.
- Applying the prestressing forces below the neutral axis induces moments which oppose those caused by externally applied loads, thus significantly reducing the deflection and tensile stress.
- Smaller cross-section is required as compared to reinforced concrete section for the same imposed loads.
- Smaller foundations required due to reduction in self-weight

Disadvantages of prestressed concrete over reinforced concrete structures are:

- The need for experienced builders.
- Initial equipment cost is very high.
- Need for experienced engineers.
- Prestressed sections are brittle sections and are less fire resistant.

1.3 TYPES OF PRESTRESSING SYSTEM

The Prestressing system is generally grouped into Pre-tensioning & Post-tensioning.

1.3.1 Pre-Tensioned Prestress Concrete

In pre-tensioned prestressed concrete, concrete is cast around steel cables while they are under tension. The concrete bond to these steel cables as it gains strength. After gaining of sufficient strength by the concrete, the ends of these steel cables are cut. By this process, compressive force is transferred to the concrete by static friction.

1.3.2 Post-Tensioned Prestressed Concrete

In post-tensioned prestressed concrete structures, prestressing force is applied to the concrete using prestressing steel cables after the concrete is placed and gained sufficient strength. The prestressing tendons are sheathed or placed in already formed ducts. Ducts can be grouted after post tensioning to protect the prestressing cables from moisture and corrosion.

The post-tensioning system is generally further grouped into un-bonded and bonded system.

1.3.2.1 Un-bonded tendons

The basic characteristic of unbounded system of post-tensioning is that it does not form a bond along its length with the surrounding concrete. The unbounded prestressing cables are mainly made of single strand of high strength steel, which is covered with corrosion resistant coating and imbedded in sheathing as shown in Fig.1.2. The force in the prestressing cables are generally transferred to concrete with the help of anchors provided at the ends. The variation in the force along the prestressing cables is largely affected by friction between strands and duct profile in the member. Therefore, it is very important to maintain the long-term integrity of the anchors throughout its service period.

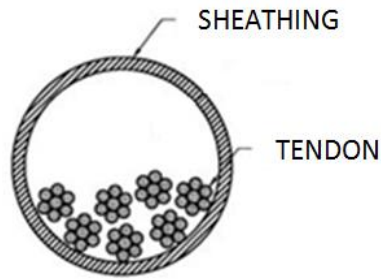


Fig.1.2: Unbounded tendon system

1.3.2.2 Bonded system

The basic characteristic of bonded system of post-tensioning is that the prestressing cables forms a continuous bond along its length with the surrounding concrete (refer Fig.1.3). The bond between prestressing cables and surrounding concrete is achieved by injecting cementitious material under pressure inside the duct after completion of stressing of the cables and transferring the loads to the anchors. This process is called grouting of the ducts. After the hardening of the cementitious material, movement of the cables within the duct is locked. Hence, the compressive force in a bonded cable becomes a function of the deformation of the concrete surrounding it.

The function of grouting is to completely fill the post-tensioned duct with high quality non-shrinkable and non-bleedable grout for the purpose of protection of the prestressing steel from failure and damage due to corrosion and friction between strands and the surrounding material and thereby endowing a serviceable structure throughout its design life.

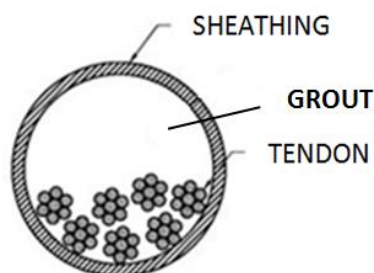


Fig. 1.3: Bonded tendon system

1.4 PRESTRESS LOSS

Prestress loss is nothing but the reduction of initial applied prestress force in the cable with respect to time. In other words, loss in prestress is the difference between initial prestress and the effective prestress that remains in a member at a particular instant of time. This loss in prestress leads to severe and critical serviceability and safety problems. If this loss in the prestress is not equal to the estimated loss in the design, the structure will not behave in a manner as envisaged during the design. Therefore, it is very important to estimate the prestress-loss by considering the fact that a prestressed concrete member should keep effective force at each significant level of loading, together with appropriate material properties for that time in the life history of the structure.

1.4.1 Type of Losses in Prestress

(a) Losses in Pre-tensioned Structures

- Elastic deformation of concrete
- Relaxation of stress in steel
- Shrinkage of concrete
- Creep of concrete

(b) Losses in Post-tensioned Structures

- No loss due to elastic deformation if all the prestressing cables are simultaneously tensioned.
- Relaxation of stress in steel
- Shrinkage of concrete
- Creep of concrete
- Friction
- Anchorage slip

Fig. 1.4 shows the losses in the prestressing force in post-tensioned structures. The present study is concerned with losses occurred over a period of time.

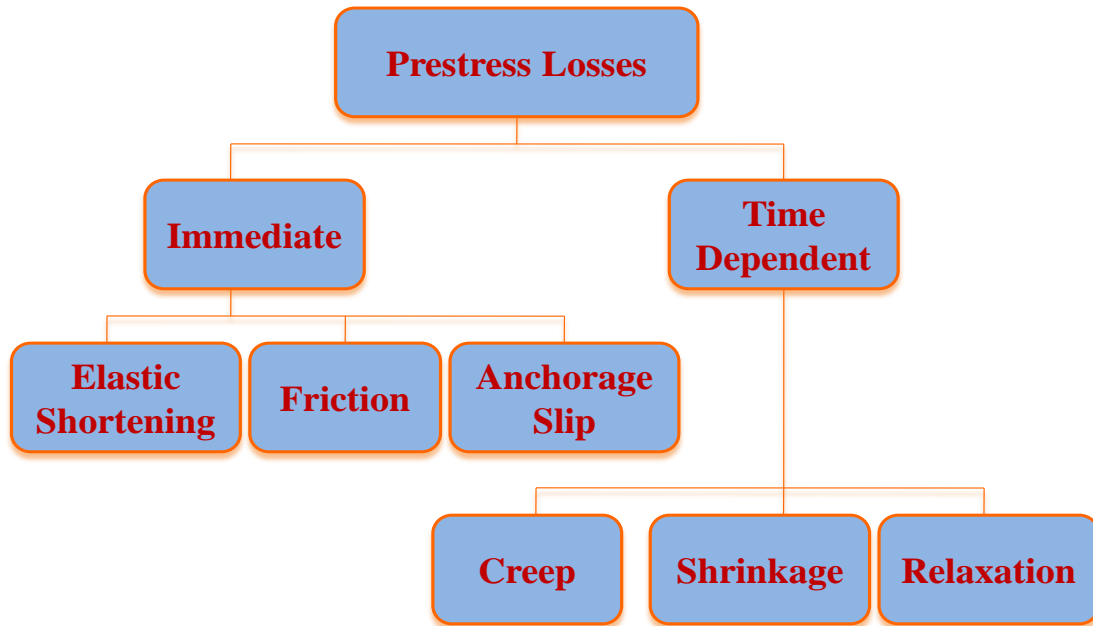


Fig.1.4: Types of Prestress Losses

Table-1.1 shows the losses in various types of prestressing systems and types of loss occurred in respective type of prestressing system.

Table-1.1: Types of losses in various prestressing systems

Type of loss	Pre-tensioning	Post-tensioning
1. Elastic Shortening	Yes	i) No, if all the cables are simultaneously tensioned ii). If the wires are tensioned in stages, loss will exist
2. Anchorage slip	No	Yes
3. Friction Loss	No	Yes
4. Creep and Shrinkage of Concrete	Yes	Yes
5. Relaxation of steel	Yes	Yes

1.5 STATEMENT OF PROBLEM

Prestressed concrete (PSC) is being widely adopted in various civil infra-structures like bridges. In search of trouble free service from pre-stressed concrete structures, lot of considerations are required at the time of construction. In the old existing bridges, durability aspect is not considered during their design. Due to this, several PSC structures develop defects during their service life. The most common problems are corrosion of reinforcing steel and pre-stressing cables, cracks development, excessive deflections, shrinkage of concrete, creep of concrete, etc. These defects may lead to loss of prestress force. It is important to note that there is no direct method to measure loss of pre-stress in existing PSC structures.

Several researchers tried non-destructive evaluation methods of vibration test to estimate the prestress loss in the PSC bridges. Based on the previous research, following is inferred:

- The loss of the prestress force in the structure results in the change in structural stiffness.
- The loss of the prestress force changes vibration characteristics of the structure.
- The change in structural stiffness can be estimated by monitoring changes in vibration characteristics of the structure.

Due to this, analytical and experimental approach, correlating prestressing force, natural frequency under assumption of conservation of energy is adopted for assessment in the present study.

1.6 OBJECTIVE OF THE STUDY

To find the relationship between natural frequency of the structure and present prestressing force in PSC structure so as to ascertain the existing prestressing force and subsequently loss of prestress.

1.7 ORGANISATION OF THESIS

The thesis has been divided in five chapters dealing with different contents of the project work. The chapters along with brief description have been mentioned here as:

Chapter-1:

It contains a general introduction of the topic i.e. loss of prestress in pre and post tensioned type prestressed concrete (PSC) structures. It also highlights the objective of the problem.

Chapter-2:

It contains the critical review on the topic of variation of prestressing forces with flexural rigidity and fundamental natural frequency of the beam. Various dynamic parameters have been studied and discussed which relates stresses due to prestress and their losses. Also, different methods for estimation of prestress forces have been reviewed.

Chapter-3:

It includes methodology of experimental as well as theoretical studies of PSC beams with prestressing cables eccentricity. Two experimental program and there process have been discussed for estimating prestress force and natural fundamental frequency. Also theoretical analysis of five different cases of PSC beams has been discussed.

Chapter-4:

It includes the results obtained from both the experimental programs i.e. for extracting present prestress force and fundamental natural frequency and also the results of theoretical studies have been discussed.

Chapter-5:

Conclusions have been drawn and scope for future research work related to findings is given in this chapter. Some more prevailing conditions are discussed for consideration for next phase of work.

CHAPTER-2

LITERATURE REVIEW

2.1. INTRODUCTION

Since, prestressed concrete has proved advantageous as compared to reinforced concrete in delaying cracks, saving of construction materials and increasing service life of structures, its uses has been increased worldwide rapidly.

However, any shortfall in the design of prestress force may lead to collapse and unexpected deformation of structure. According to many researchers, any change in the structural property over a period of time i.e. mass, stiffness and damping will reflect the damage in the structure. This damage can be ascertained by knowing various vibrational properties such as natural frequency, flexibility, mode shapes etc. of the structure. Therefore, by analysing the various vibration characteristics of the structure, one can roughly estimate the present prestressed force in the structure.

2.2 REVIEW OF PREVIOUS RESEARCH PAPERS

Kim and Stubbs appraised the impact of modal uncertainty on the accuracy of damage prediction of a non-destructive damage detection technique when employed on a model plate girder. The three uncertainty types used in the study were, uncertainty involved in the selection of damage detection methods, uncertainty in the stiffness parameter and the uncertainty in the mode shapes.

The relationship between modal uncertainty and the non-destructive damage detection accuracy obtained by them are as given below:

- The uncertainty due to selection of Euler Bernoulli beam model as the damage detection model had relatively small effect on damage localization error and the model selection had a strong effect on prediction of location that were not damaged.
- Uncertainty in mode shapes had relatively strong effect on damage localization error.
- Uncertainty in stiffness parameter has no effect on non-destructive damage detection accuracy.

RDSO (2001) presented a report on instrumentation techniques to monitor loss of prestress in which the force had been estimated in prestressing cable using Vibrating Wire (V.W.) Load Cells and V.W. Strain Gauges. It had been summarized that V.W. Load Cell system are suitable for new construction and not for existing bridges, whereas V.W. Strain Gauge system is suitable both for new as well as existing bridges.

Ren et al (2002) proposed a damage identification technique which is based on changes in mode shape and frequency of vibration for predicting severity and damage location. This damage identification technique provided exact location and severity of the damaged elements.

Kim et al (2003) prepared a system identification model to calculate the changes in natural frequencies of the prestressed concrete bridges due to various prestress forces. To identify the prestress loss in PSC bridges, an inverse solution algorithm is also formulated using the changes in natural frequencies.

By applying the methodology to the test structure, it was observed that at different stages, the predicted natural frequencies and measured frequencies are comparable.

Jain et al (2003) studied the variation in natural frequency with respect to the prestress loss and structural cracks. They concluded that the theoretical and observed frequencies for the rectangular beam show similar trends but for scaled bridge model, they showed high variation that might be due to the difficulties in exactly estimating the flexural rigidity of the model, or due to other structural consequences.

Yaoting and Ruige aimed to determine a relation between prestressing force and natural frequency. For this purpose, a dynamic test on bonded and unbonded prestressed concrete beam was carried out. The dynamic experiment indicated that the natural frequency increases with increase of prestressing forces. Also a theoretical study using dynamic performance of the beam was conducted by treating the beam as orthotropic material and the results of first mode of frequency is found to be quiet satisfactory with experimental results.

Park et al (2007) presented a vibration based method in PSC girder bridges to simultaneously predict prestress loss and flexural crack location. By applying the proposed approach to the test structure, it was observed that the experimental results do not perfectly match with the predicted results; however, those results show similar trends in the prestress loss prediction in the PSC beam with external unbonded prestressing cables. Also, from the results of prestress-loss prediction in the PSC girder with an internal unbonded prestressing cable, the experimental results do not perfectly match with the predicted results; however, those results show similar trends except the prediction results for the mode-2 (refer Fig.2.1), where mode-1 and mode-2 are the vibration mode at which losses are calculated.

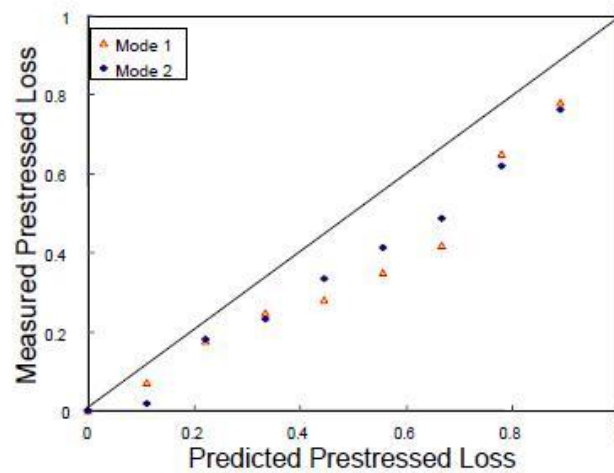


Fig.2.1: Prestress-loss prediction result for PSC girder [Park et al (2007)]

Also, from the results of locating flexural crack for PSC girder using mode shape based method, the real damage location in case of damage-1 is correctly predicted. However, the real damage location in the case of damage-2 is not correctly predicted (refer Fig.2.2), where damage-1 and damage-2 are the levels of damage at respective prestress loss.

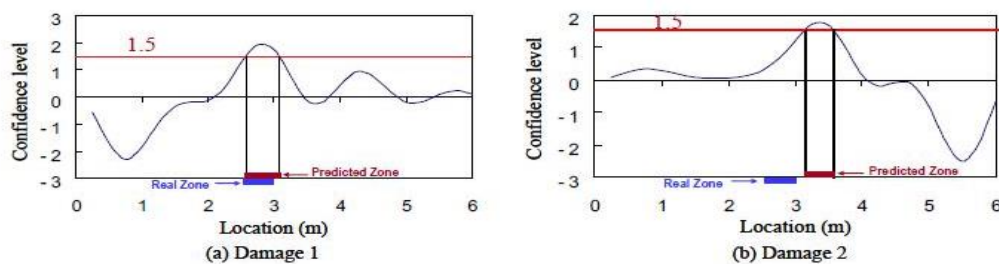


Fig.2.2: Results of damage location for each damage case in PSC girder [Park et al (2007)]

Kim et al (2008) conducted experimental and theoretical study to find out damage due to change in prestressing force in the cable. For this, first two sensing mechanism i.e. acceleration and electro-mechanical impedance were used for vibration characteristics. Also, to extract features from those signals, four acceleration based algorithms and three impedance based algorithms were selected. Next, the working of those methods was evaluated for different prestress loss cases using a large scale PSC girder by both commercial instrumentation and a wireless smart sensor node.

From the performance evaluation of the four acceleration based methods, the frequency-response-ratio assurance criterion and the correlation coefficient of frequency response functions successfully showed the occurrence of damage in most of the prestress loss cases. From the performance evaluation of the three impedance based methods, the correlation coefficient of impedance signatures and the root-mean-square deviation successfully showed the occurrence of damage in most of prestress loss cases.

From this study, they concluded that the vibration based damage monitoring algorithms were suitable for the smart sensor nodes in order to provide a warning for the occurrence of prestress loss in PSC girder bridges.

Barr et al (2008) performed testing on instrumented five precast prestressed girders made with high performance concrete (HPC) at the concrete age of three years, in order to monitor the prestress losses for short span i.e. span-1 and for long span i.e. span-2. The observed values of prestress losses were compared with values calculated using the AASHTO LRFD Specifications (AASHTO 2004) The study led to the following conclusions:

- If the calibrated elastic modulus had been used in the Span-2 design and the girders were analysed as continuous beams for differential shrinkage, the difference between the measured total losses and the calculated losses using the NCHRP method would have been within 10%. If the calibrated elastic modulus was used with the AASHTO method, the total losses would have been over 30% higher than the measured losses.
- For the Span-1 girders, the AASHTO LRFD method was within 2% of the measured losses, whereas the NCHRP 18-07 losses were about 22% smaller. The

closeness of the AASHTO method is attributed to the lower stresses used in Span-1, while, the NCHRP 18-07 losses are based on highly stressed HPC concrete.

- The NCHRP method was closer to estimating the elastic shortening losses in comparison to the AASHTO method. On average, the observed elastic shortening losses were found to be 21% higher than those calculated using AASHTO and 11% lower than those calculated using the NCHRP method.

Materazza et al (2009) conducted a sensitive study on the effect of prestressing on dynamic properties notably for Eigen frequencies of prestressed concrete. Different prestressing techniques as well as several material properties had been deliberated. A Finite Element Method (FEM) based modelling of the structure had been done and it was observed that for accurate results, particular attention should be paid on the modelling of structure elements when using dynamic methods within framework of structure identification and damage detection.

Khoshnoudian and Esfandiari presented a universal algorithm for damage evaluation of structure which was based on parameter estimation method, using finite element and measured modal response of the structure.

It was considered that damage is due to localized reduction of structure stiffness. The results showed, the method provides good ability to detect any damage of structure in the existence of errors in the acquired data.

Lan et al (2012) designed a novel smart steel strand which was based on optical fiber Brillouin sensing technology in order to monitor full-scale prestress loss of prestressed structures. For verification of full scale prestress loss, monitoring of damaged beams using the smart steel strands, laboratory tests of two similar beams with different damages were used. BOTDA (Based fibre optic distributed strain) sensors used to obtain prestress loss. The results concluded that the smart steel strands used were sufficiently rugged and simple to install using normal equipment and also showed that the smart steel strand had a sensitivity coefficient of 43.98 $\mu\epsilon/kN$, linearity of 3.9% FS, repeatability of 1.7% FS, overall accuracy of 3.3% FS, and hysteresis of 1.3% FS.

At the stage of the first crack, the time dependent prestress loss of beams did not changed significantly with time. Also at the stage of maximum allowable crack

width, the prestressing losses in beam increased with time but during the initial stage, a higher prestress loss rate was observed and the rate of prestress loss reduces gradually after that.

Halvonik et al (2013) conducted an experimental program which was aimed on the monitoring of the prestress losses in the beams cast using normal concrete (40/50 MPa) and high performance concrete (70/85 MPa). In this experimental program, same prestressing force was applied on both the beams. To measure these prestress forces, an electromagnetic sensor was embedded on the pre-tensioned strands of the beams. The result showed that the material properties affecting the prestress loss due to creep, shrinkage and elastic shortening of concrete were superior for HPC as compared to high quality normal concrete.

Hao Li et al (2013) carried out a numerical simulation by making use of the dynamic responses from moving vehicular loads in order to identify the magnitude of prestressing force in a bridge. For this purpose, a prestressed bridge was modelled using four-node iso-parametric flat shell element with the transverse shearing deformation in the finite element model and the vehicle is modelled as a multiple degree of freedom system. Two numerical examples of a single-span prestressed Tee beam and the two-span prestressed box girder bridge were studied. The influence of road surface roughness, measurement noise and speed of vehicles were also taken into consideration.

Two numerical simulations show that the proposed method was correct and efficient for prestress force identification. Study also shows that the speed of the moving vehicle had little effect on the identified results and the artificial measurement noise did not had significant effect on the identified results, but larger identified error was observed under a weak road condition.

Wang et al (2013) conducted an experimental as well as theoretical analysis in order to find the variation of flexural rigidity for post tensioned prestressed concrete beams. In their study, two parameters i.e. eccentricity and force on the beam were used to indicate the results. The authors did an experiment with simply supported beams with parabolic as well as straight profile of prestressing cables for the theoretical purpose. The natural frequency of axial-loaded concrete beam decreases

with increasing applied compressive force, and the natural frequency of tensioned cable increases with increasing tensile force. However, the variation of natural frequency of prestressed concrete beam (PCB) consisting of concrete and cable has rarely been discussed based on both the rigorous mathematic model and experimental results. In this study, a testing program was conducted and Rayleigh's method was used to derive an approximate equation for computing natural frequency. The results indicate that (1) the natural frequency Rayleigh's method was used. The results of the study indicates that the natural frequency decreases with increasing Prestress force for prestressed concrete beams with parabolic eccentricity and had no change with straight eccentricity of the beam. Also a modified computed method for finding the effective moment of inertia of prestressed concrete beam had been developed.

2.3. TECHNIQUES OF CALCULATING PRE-STRESSING FORCE AND LOSS

2.3.1 Vibration Based Damaged Detection Technique

2.3.1.1 Prestress loss prediction model developed by Kim et al (2003)

Kim et al (2003) developed a prediction model for a simply supported PSC beam with a straight concentric tendon. Figure 2.3 shows a tension strength model of PSC beam, for which a tendon is initially stretched and anchored to introduce pre-stressing effect.

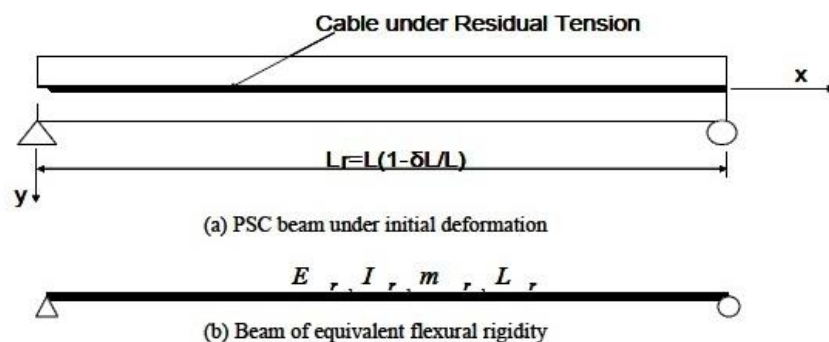


Fig.2.3: Tensile Strength Model of PSC Beam

The governing differential equation for the beam is expressed by:

$$\frac{\partial^2}{\partial x^2} \left(E_r I_r \frac{\partial^2 y}{\partial x^2} \right) + m_r \frac{\partial^2 y}{\partial t^2} = 0 \quad \dots \quad 2.1$$

Where $E_r I_r$ is the flexural rigidity of PSC beam section and m_r is mass per unit length of PSC beam.

The composite flexure rigidity and mass can be evaluated as:

$$E_r I_r = E_c I_c + E_s I_s, m_r = \rho_c A_c + \rho_s A_s \quad \dots \quad 2.2$$

Where, 'c' corresponds to the contribution of concrete and, 's' corresponds to the tendons.

The equivalent flexural rigidity of tendon is deduced from mode characteristics of the cable and the equivalent beam model. It is expressed by:

$$E_s I_s = \left(\frac{L_r}{n\pi} \right)^2 N \quad \dots \quad 2.3$$

Where, 'N' is the prestress force which is applied at its anchoring edges.

On substituting these equations, and applying appropriate boundary conditions to Eq.2.1, leads to n^{th} natural frequency of the residual tension model as follows:

$$\omega_n^2 = \left(\frac{n\pi}{L_r} \right)^4 \frac{1}{m_r} \left(E_c + \left(\frac{L_r}{n\pi} \right)^2 \right) N \quad \dots \quad 2.4$$

2.3.1.2 Mode shape based crack detection method by Kim et al. (2003)

Kim et al. (2003) considered a homogeneous, uniform cross-sectional one-dimensional beam with NE element and N nodes. Assume that the input output relationship of the beam is linear. Assuming a solution of the associated dynamic Eigen value problem, the i^{th} modal stiffness, K_i , of the beam is given by:

$$K_i = \int_0^L k(x) [\phi_i''(x)]^2 dx \quad \dots \quad 2.5$$

Where, $\phi_i(x)$ is the mode shape of i^{th} modal vector and $k(x)$ is the bending stiffness of the beam. The contribution of the j^{th} element to the i^{th} modal stiffness, k_{ij} , is given by;

$$k_{ij} = k_j \int_j^0 [\phi_j''(x)]^2 dx \quad \dots \quad 2.6$$

Where, k_j is the stiffness of the j^{th} element and the integral is over the beam length.

2.3.1.3 Acceleration based method [Kim et al (2008)]

Damage detection can be done using frequency response of the structure. The basic ideology behind it is that frequency responses are the functions of the structural properties such as mass (m), damping (c) and stiffness (k). Due to damage in the structure, the properties of the structure changes, this in turn, changes the frequency responses of the structure.

The frequency response function, $H(f)$ for the relation between input force and output response is defined as follows:

$$H(f) = \frac{V(f)}{U(f)} = \frac{1}{-m(2\pi f)^2 + ic(2\pi f) + k} \quad \dots \quad 2.7$$

Where, $U(f)$ and $V(f)$ are force and displacement transformed into frequency domain respectively. The symbols m , c and k are mass, damping and stiffness of the structural system respectively. Natural frequency can be estimated by reading peak values of spectrum estimated from Fourier transform.

2.3.1.4 Impedance based method [Kim et al (2008)]

Impedance based health monitoring techniques uses piezoelectric materials as sensors and actuators. An electric field is generated when a piezoelectric material is mechanically strained. Or we can say, its shape gets changed when an electrical field is charged. Also, the materials have unique molecular structures, which allow bidirectional coupling between electric field and strain; hence, they are helpful for self-sensing, power harvesting, and SHM applications.

In this process, an active material is stated by its short circuited mechanical impedance, which is powered by current or voltage. The host structure is described by the effect of mass, stiffness, damping, and boundary conditions. The electrical admittance (the inverse of electro mechanical impedance) of the patch, $Y(\omega)$ (units Siemens or ohm^{-1}), is a combined function of the mechanical impedance of the host structure $Z_s(\omega)$, and that of the piezoelectric patch, $Z_a(\omega)$, when a piezoelectric patch is surface bonded to a structure.

$$Y(\omega) = i\omega \frac{wl}{t_c} \left[(\epsilon_{33}^T - d_{3x}^2 Y_{xx}^E) + \frac{Z_a(\omega)}{Z_a(\omega) + Z_s(\omega)} d_{3x}^2 Y_{xx}^E \left(\frac{\text{tankl}}{kl} \right) \right] \quad \dots \quad 2.8$$

Where, Y_{xx}^E is the complex Young's modulus at zero electric field; ϵ_{33}^T is the dielectric constant of piezoelectric wafer; d_{3x}^2 is the piezoelectric coupling constant in the x direction at zero stress; k is the wave number that depends on mass density and Young's modulus of the piezoelectric material; and w , l , and c are the width, length, and thickness of the piezoelectric transducer respectively.

Equation 2.8 states that the electrical impedance is directly related to mechanical impedance of the structure. The first and second term denotes the capacitive admittance of the free piezoelectric patch and mechanical impedance of both piezoelectric patch and the host structure respectively.

When the damage occurs to a structure, its mechanical impedance gets changed and hence, any change in the electric impedance signature is specified to damage or changes in the structure.

2.3.1.5 Rayleigh's Method [Wang et al (2013)]

This method is used to determine the approximate value of fundamental natural frequency. This method is based on the principle that if the system is conservative, the maximum kinetic energy T_{\max} is equal to the maximum potential energy V_{\max} . By equating both T_{\max} and V_{\max} , the fundamental natural frequency ω can be obtained.

The kinetic energy of Prestressed Concrete Beam is expressed as:

$$T = \frac{1}{2} \int_0^l \dot{y}^2 dm = \frac{1}{2} \int_0^l \dot{y}^2 \rho(x) dx \quad \dots \quad 2.9$$

Where, $\rho(x)$ is mass per unit length, y is the harmonic moving equation assumed as $y=w(x)\cos\omega t$. $w(x)$ is assumed as vertical deformed shape function of beam. Then the max kinetic energy can be expressed as

$$T_{\max} = \frac{\omega^2}{2} \int_0^l \rho(x) [w(x)]^2 dx \quad \dots \quad 2.10$$

By ignoring work done by shear forces, the potential energy of the deformed beam can be expressed as:

$$V = \frac{1}{2} \int_0^l M d\theta \quad \dots \quad 2.11$$

Where M is the bending moment expressed as:

$$M = EI \frac{\partial^2 y}{\partial x^2} = EI \frac{\partial^2 w}{\partial x^2} \cos \omega t,$$

$$\theta = \frac{\partial y}{\partial x} = \frac{\partial w}{\partial x} \cos \omega t \text{ and } d\theta = \frac{\partial^2 w}{\partial x^2} \cos \omega t \quad \dots \quad 2.12$$

By substituting values of M & θ in Eq. (2.11), we get the maximum value of V as:

$$V_{\max} = \frac{1}{2} \int_0^l EI \left(\frac{\partial^2 w}{\partial x^2} \right)^2 dx \quad \dots \quad 2.13$$

By putting $T_{\max} = V_{\max}$, the first fundamental natural frequency ' ω ' can be obtained as :

$$\omega_1^2 = \frac{\frac{1}{2} \int_0^l EI \left(\frac{\partial^2 w}{\partial x^2} \right)^2 dx}{\frac{1}{2} \int_0^l \rho(x) [w(x)]^2 dx} \quad \dots \quad 2.14$$

2.3.1.6 Simply Supported Beam with Parabolic duct profiles:

Natural frequencies of bridges have certain sensitivity to prestressing force, so the identification of effective prestressing force based on bridge's natural frequencies, is an effective method. The behaviour of prestressed beam can be described as a combination of two substructures: a compressive concrete beam and a tensioned cable. The dynamic equilibrium equations of the two sub systems are established using Rayleigh Method of structural vibration analysis. Based on the coupling analysis and processing of the vibration equation of sub system, a calculation method of natural frequency of beam is derived. Consider a Simply Supported Beam with parabolic prestressing cable profile 'e(x)' and length 'L'. The beam is subjected to a compressive axial force P in kN as shown in Fig.2.4.

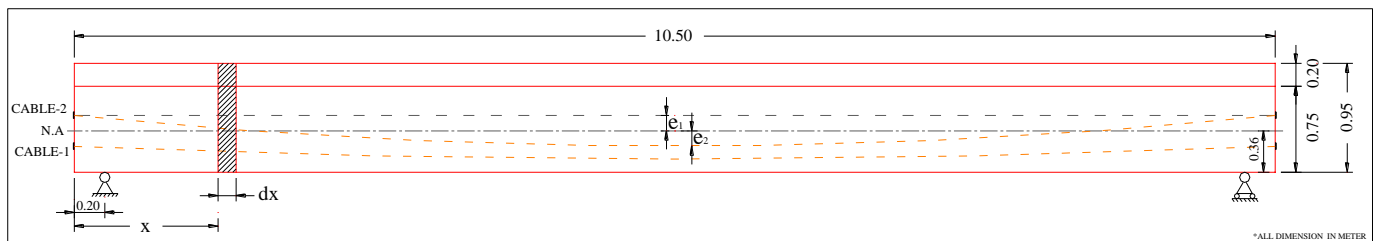


Fig.2.4: Layout of Prestressed simply supported beam with parabolic prestressing cables profile

For simply supported beam,

$$Y(x) = \frac{\gamma_0}{24EI}(L^3x - 2Lx^3 + x^4)$$

$$M(x) = \frac{\gamma_0}{2}(Lx - x^2)$$

where,

M(x) is the bending moment of beam at a distance 'x' from the support

Y(x) is the vertical deformed shape function of the beam at 'x' from the support

The flexure rigidity EI for combined section = $(E_c I_c + E_s I_s)$

Where 'c' stands for concrete and 's' for steel.

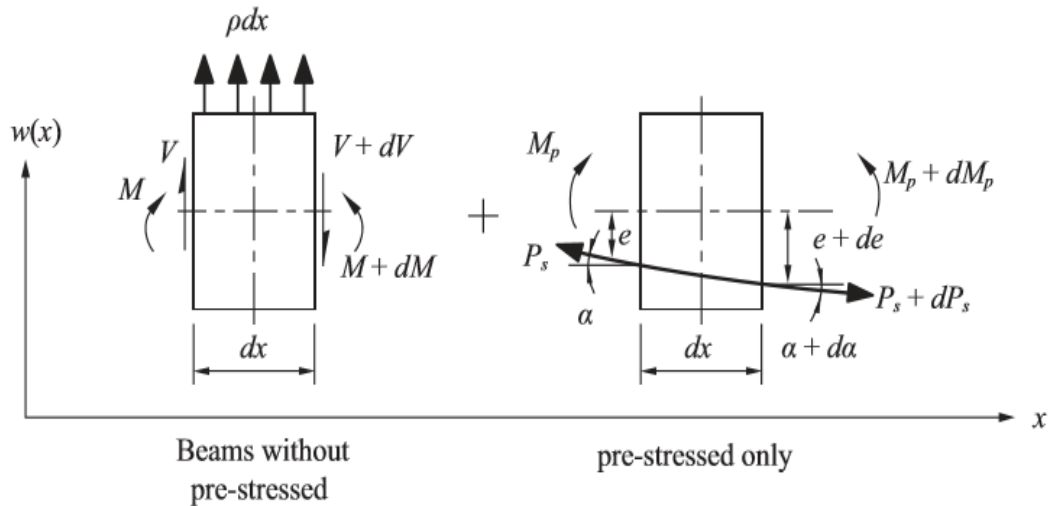


Fig.2.5: Element of Beam with and without Prestressing Cables

Eccentricity of tendon at any point x for parabolic profile is:

$$e(x) = \frac{4e_0}{L^2} (x^2 - Lx) + C(x^2 - Lx) \quad \dots (2.15)$$

Where $C = \frac{4e_0}{L^2}$

Then,

$$\frac{de}{d\alpha} = \tan \alpha = C(2x - 1) \sim \alpha$$

Where α is the curvature of the tendon profile

$$de = \alpha dx$$

$$\frac{d\alpha}{dx} = \frac{d^2e}{dx^2} = 2C$$

Therefore,

$$d\alpha = 2C dx \quad \dots (2.16)$$

For beams with parabolic prestressing tendons, an additional moment dM_p will be generated due to prestressing force at distance 'x' as shown in Fig-2.5. So by force equilibrium,

$$dM_p + (P + dP)(e(x) + de) \cos(\alpha(x) + d\alpha) - P e(x) \cos \alpha(x) - P \sin \alpha(x) dx = 0$$

$$\text{Hence, } dM_p = P e(x) \alpha(x) d\alpha - P de + P \alpha(x) dx - e(x) dP \quad \dots (2.17)$$

Where dM_p is the additional moment induced by prestressing force at distance 'x' as shown in Fig.2.4 and P is prestressing force, dP is the change in prestressing force which will increase in one side and decrease in the other side for beams with symmetrical tendon and prestress at both ends. Therefore the effects of dP will be vanished each other in the process of integration and can be neglected and the modified term for dM_p will be:

$$dM_p = Pe(x) \alpha(x) dx - Pde + Pa(x) dx \quad \dots (2.18)$$

The terms $e(x)$ is the eccentricity of tendon at x. For beams with parabolic tendon with eccentricity, the profile of parabolic tendons as shown in Fig.2.4 is:

$$e(x) = \frac{4(e_1 + e_2)}{L^2} (L^2 - Lx) - e_1 \quad \dots (2.19)$$

$$\text{Taking } C = \frac{4(e_1 + e_2)}{L^2}$$

$$e(x) = C (L^2 - Lx) - e_1 \quad \dots (2.20)$$

$$\frac{de}{dx} = \tan \alpha = C (2x - L) \cong \sin \alpha = \alpha$$

Where α is the curvature of tendon profile

$$\therefore de = \alpha dx$$

$$\frac{d\alpha}{dx} = \frac{d^2e}{dx^2} = C (2x - L)$$

$$d\alpha = C (2x - L) dx \quad \dots (2.21)$$

Now considering Eq-(2.17) for evaluation,

P = Prestressing force

$$e(x) = C(x^2 - Lx) - e_1$$

$$\alpha(x) = \alpha = C (2x - L)$$

$$d\alpha = 2C dx$$

$$de = C (2x - L) dx$$

Putting values of 'P, $e(x)$, $\alpha(x)$, $d\alpha$ & de ' in equation as derived above, the Eq-(2.18) can be derived as:

$$dM_p = 2PC^2(Cx^2 - CLx - e_1)(2x - L)dx, \text{ and the additional moment } M_x \text{ at 'x'}$$

$$M_x = \int_0^x dM_p = 2PSC^2 \left(\frac{2Cx^4}{4} - LCx^3 + \frac{CLx^2}{2} - e_1x^2 + e_1Lx \right) \quad \dots (2.22)$$

For simply supported non-prestressed concrete beams, the shape function in vertical direction $w(x)$ is assumed as equation:

$$w(x) = K(L^3x - 2Lx^3 + x^4)$$

Where $K = \frac{\gamma_0}{24EI}$, γ_0 is the unit weight of beam and 'x' is the section position distance from the original point.

Finding 1st derivative of $w(x)$ with respect to x

$$w'(x) = K(L^3 - 6Lx^2 + 4x^3)$$

Finding 2nd derivative of $w(x)$ with respect to x

$$w''(x) = K(12x^2 - 12Lx) \quad \dots (2.23)$$

For V_{max} :

$$\text{Then } V_{max} = \frac{1}{2} \int M(x) d\theta$$

$$V_{max} = \frac{1}{2} \int_0^L EI (w''(x))^2 dx + \frac{1}{2} \int_0^L M_x w''(x) dx \quad \dots (2.24)$$

Putting values of $w''(x)$, we get

$$\begin{aligned} V_{max} = & \frac{1}{2} \int_0^L EI (12K)^2 (x^2 - Lx)^2 dx \\ & + \frac{1}{2} \int_0^L (2PC)^2 \left(\frac{2Cx^4}{4} - \frac{3LCx^3}{3} + \frac{CL^2x^2}{2} - e_1x^2 + e_1Lx \right) [K(12x^2 \\ & - 12Lx)] dx \end{aligned}$$

$$V_{max} = \frac{12}{5} K^2 EIL^5 + 12PC_1^2 K \left(\frac{9}{70} C_1 L^7 - \frac{3}{10} e_1 L^5 \right) \quad \dots (2.25)$$

2.3.1.7 Mode shape curvature/strain mode shape changes [Kim et al (2014)]

In this method, it was assumed that the root for detection of damage were pre and post-damage eigenvectors. Thereby the mode shape curvature for the beam in the undamaged and damaged condition can then be estimated numerically from the displacement of mode shapes.

For a beam cross section, subjected to a bending moment $M(x)$ and flexure rigidity EI , the curvature $K(x)$ at any location x is given by:

$$K(x) = \frac{M(x)}{EI} \quad \dots \quad 2.26$$

There will be a change in the actual stiffness of the beam due to the damage undergone in the beam with certain time duration with the given moment applied to the damaged and undamaged structure, which will lead to an increase in curvature. Thus the existence and amount of damage can be predicted by estimating the amount of change in the mode shape curvature. The curvatures are often evaluated using the central difference approximation.

$$K = \frac{\varphi_{(j+1)i} - 2\varphi_{ji} + \varphi_{(j-1)i}}{l^2} \quad \dots \quad 2.27$$

With i being mode shape number, j the node number, φ_{ij} is the modal displacement of the coordinate j at mode i . l is distance between the nodes.

The mode shape curvature criterion may be defined as the difference in absolute curvatures (Δ) of the undamaged and damaged structures, for each mode, and may be represented as:

$$\Delta = \kappa_{ud}(x) - \kappa_d(x) \quad \dots \quad 2.28$$

At a certain location of damage, the value of mode shape curvature was significantly higher than the ones at other locations. Based on the curvature difference values of measured data of damaged and undamaged structures, the damage location of the structure could be spotted.

2.3.1.8 Methods based on dynamically measured flexibility

The main principle of vibration based damage detection methods is that the damage alters the mass (m), stiffness (k) and damping (c) properties of a structure, which in turn endure the structural modal parameters. Stiffness change due to damage is a promising factor in prediction of damage location, since any change in elemental stiffness throughout the stiffness matrix can lead to structural damage. Unfortunately, derivation of a fairly accurate stiffness matrix based on a few lower frequency measured modal data is very difficult to achieve. However its inverse, i.e. flexibility matrix, can be approximated using the first few measured modal data due to the inverse relationship to the square of modal frequencies

2.3.2 Distributed Optical fiber sensing technique

Optical fiber sensors have been developed for a number of years and many optical fiber-based sensing techniques have been established for structural health monitoring because of their advantages such as resistance to electrical noise, long-term measurement stability and resistance to corrosion.

2.3.3 Instrumentation techniques

There is no direct method to measure loss of prestress in the existing structures. However, loss of prestress in the existing structures can be predicted by knowing the changes in stress levels in pre stressing cables which can be periodically measured, if some sensors are installed during the construction. These sensors may be Vibrating Wire Load Cells, Vibrating Wire Strain Gauges, Wire Tension Meter (for externally prestressed structures) etc.

Prestressing force can be indirectly estimated by knowing different dynamic properties of the structure like stiffness, flexibility, mode shapes, frequency etc.. These properties could be determined with the help of various instrumentation techniques.